Recovery of Aluminium from Metal Pads in Shutdown Aluminium Electrolysis Cells

Samuel Senanu[1], Martin Syvertsen[2], Erik Koren[3] and Arne Petter Ratvik[4]
1, 2, 4. Senior Research Scientist
3. Research Scientist
SINTEF Industry, Trondheim, Norway
Corresponding author: samuel.senanu@sintef.no
https://doi.org/10.71659/icsoba2024-al065

Abstract

Remaining aluminium mixed with cryolite from shutdown electrolysis cells, commonly called metal pads, have been collected from two aluminium smelters in Norway for process developments to recover the aluminium metal. Two samples of metal pads were collected from the smelters. One sample was pre-processed via mechanical cleaning to reduce the cryolite content. Both pre-processed and non-pre-processed metal pads were heated to temperatures of 750 °C and 830 °C in a crucible placed in an electric furnace. A Fourier-transform infrared spectroscopy, FTIR, gas measurement instrument was used to characterise the off gases. Results from the aluminium recovery tests showed a higher productivity and lower HF emissions for the pre-processed metal pads relative to the non-pre-processed metal pads. Furthermore, the importance of water vapour to the formation of HF during the heat treatment was investigated using a humidifier.

Keywords: Metal pads, Pre-processing, FTIR, Shutdown, Aluminium, Cryolite.

1. Introduction

The global aluminium industry produced ca. 70.6 Mt of primary aluminium using the Hall-Héroult (HH) technology in 2023 [1]. The HH technology is based on an electrochemical reduction in an electrolysis cell at about 960 °C to produce aluminium. The electrolysis cell consists of carbon anodes that conduct electricity and are consumed during the production process, a molten cryolitic based electrolyte that conducts electricity and dissolves alumina, a molten aluminium metal pad that acts as the electrochemical cathode, a cathode lining consisting of carbon cathode blocks (with different degrees of graphitization) rodded with current collector bars for conducting electricity, refractories and insulation materials, and a side wall material. The carbon cathode blocks together with the current collector bars, refractories, insulations, side wall materials are usually arranged in a rectangular steel shell that vary from 9 to 18 m long, 3 to 5 m wide and 1 to 1.5 m deep. The operating cavity depth after installation of all lining materials is about 0.4 to 0.5 m [2]. The molten electrolyte and aluminium metal pad are usually kept at a height of 15-20 cm and 10-20 cm, respectively, during the electrolysis process [2, 3]. Two types of anode technologies exist in the industry; Søderberg technology, where the carbon anodes are baked in the reduction cell during electrolysis, and prebaked technology, where the carbon anodes are baked at a separate unit and transported to the electrolysis cell [2, 4]. Figure 1 is a sketch of the electrochemical reduction cell using the prebaked anode technology.

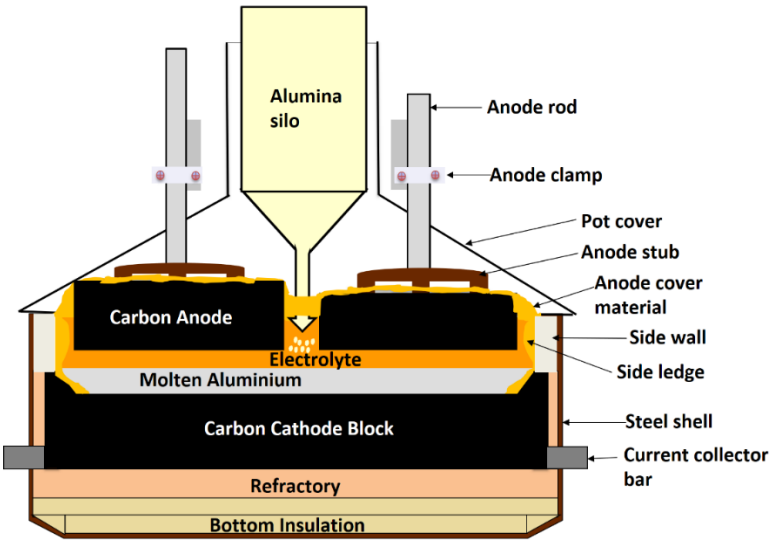

Figure 1. Electrochemical reduction cell using prebaked anode technology [5].

The lining materials within the electrolysis cell will over time degrade or in some extreme conditions fail leading to the shutdown of the cell [6]. The time from which an electrolysis cell is started to when it must be decommissioned is referred to as the pot age. The pot age varies a lot and can be from a few hundred days to over 3000 days [7, 8]. Prior to shutting down an electrolysis cell due to lining degradation or failure, operators at smelters attempt to tap as much molten aluminium metal out of the pot as possible. However, the amount of metal tapped varies a lot based on the experience of the operators and other factors such as potholes and other deformations on the cathode lining. Thus, quite a considerable amount of metal is sometimes left in shutdown cells. Considering the number of electrolysis cells that are shut down daily at the different smelters across the industry, this translates into many tonnes of aluminium left untapped. A few days after shut down, the electrolysis cell cools down causing all remaining electrolyte (mostly cryolite) and aluminium metal to freeze [6, 9]. The densities of molten aluminium and molten cryolite at the operation conditions are ca. 2.3 g/cm^3 and 2.1 g/cm^3, respectively [2]. The small density difference between the two liquids and the close contact with each other results in the frozen metal being partly mixed with frozen cryolite after the cooling preceding shutdown. Thus, the frozen metal pad is always observed together with frozen cryolite and can in some cases be mixed with but in most cases found only on the surface of the metal. This paper describes the recovery of aluminium from the metal pads collected from two smelters in Norway.

2. Experimental

Metal pads were collected at two different aluminium smelters in Norway, denoted as Smelter 1 and Smelter 2. Figure 2a shows the metal pads from Smelter 1, which were used “as collected”. The metal pads from Smelter 2, shown in Figure 2b, were pre-processed by mechanical cleaning using pneumatic hammers to remove most of the frozen cryolite. Additionally, the metal pads from smelter 2 contained alumina balls which had been used to seal a hole created in the cathode lining during operation to prolong the lifetime of the cell.

A resistance heated furnace was used to heat the crucible employed in all the melting tests. In the first melting test using batch 1 from smelter 1, the metal pads were added to an empty crucible inside the furnace before the pre-heating started. The furnace was then pre-heated and held at a temperature of ca. 830 °C.

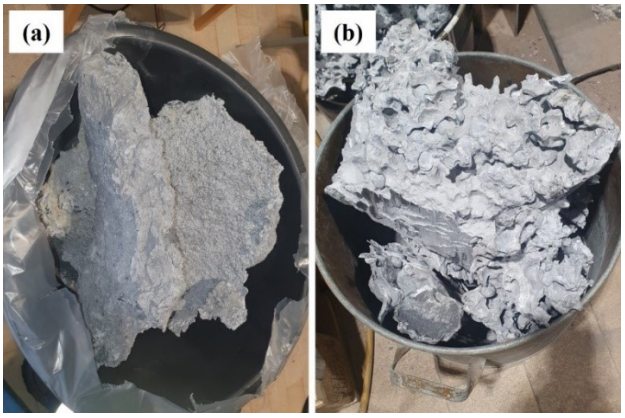

Figure 2. Metal pads collected at (a) Smelter 1 "as collected" and (b) Smelter 2 "pre-processed".

For the tests involving melting pre-processed metal pads from smelter 2, hereby called test number 2 and 3, the pre-processed metal pad was divided into two batches of 14.7 kg and 22.7 kg, respectively. The first batch weighing 14.7 kg was used for test number 2 and the second batch weighing 22.7 kg was employed for test number 3. Test number 3 involved melting the pre-processed metal pad in 60 kg pre-melted aluminium. An overview of the different metal pad melting tests performed is given in Table 1 below.

Table 1. Overview of the performed tests.

Test no.	Batch	Pre-processed	Pre-melted Aluminium	Weight of metal pad (kg)	Temperature in crucible (°C)
1	Smelter 1	No	No	74.2	830
2	Smelter 2	Yes	No	14.7	830
3	Smelter 2	Yes	Yes	22.7	750

For the test involving immersing metal pads in molten aluminium, the metal pads were added in three batches, at intervals of 30 minutes, to ensure that the melt temperature was above 745 °C. The temperature inside the crucible was monitored with a thermocouple. The off-gas was analysed using Fourier-transform infrared spectroscopy, FTIR. Also, during the melting tests using metal pads from Smelter 1, a humidifier was used to study the effect of water vapour on the formation of HF. The metal pads and bath residue after melting were analysed using powder X-ray diffractometry, XRD. Figure 3 shows the main components of the laboratory set up employed for the melting tests.

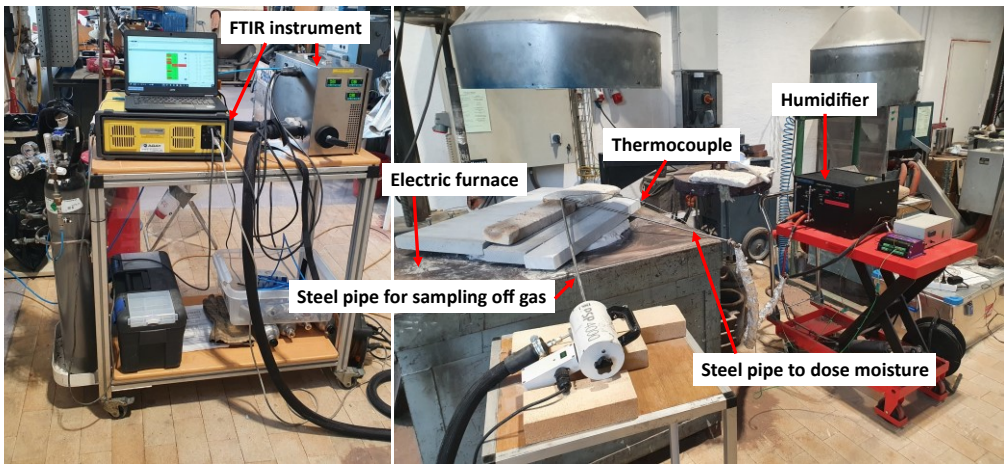

Figure 3. Setup for the metal pad melting test showing the FTIR and humidifier.

3. Results

3.1 Test 1: Melting of Non-Pre-Processed Metal Pad

Figure 4a shows the metal pad during melting. It took several hours to melt the metal pad, and a significant amount of bath remained after the test, as shown in Figures 4b and 4c. The weight of the residual bath was 59.1 kg. The tapped aluminium shown in Figure 4d, had a weight of 17.5 kg, giving an output of 24 %. The total weight of the residual bath and produced aluminium was 76.6 kg, which is higher than the initial weight of the metal pad (74.1 kg). A whitish and powdery material was observed on the surface of the chunk of frozen cryolite shown in Figure 4b. This whitish material was observed at the same location that aluminium had earlier on been observed. The sample was analysed using powder X-ray diffractometry.

Figure 4. a) Metal pad during melting in crucible at 830 °C. b) Removal of bath residue from crucible. c) Bath residue after test. d) Tapping of aluminium.

The temperature in the test crucible, content of HF and water vapour in the off gas as a function of time are shown in Figures 5 and 6. A close relationship can be observed between the HF and water vapour content in these figures. A water vapour content of 1.5 % is observed to be sufficient to produce HF. It was also observed that HF formation occurs at a higher temperature than room temperature. This is shown by the green dotted lines in Figure 5. Despite the presence of water vapour, there was no HF formation until the temperature reached ca. 450 °C. Once the required temperature is reached, HF formation is observed to be very dependent on the water vapour content with the level increasing dramatically when the water vapour content was increased using the humidifier. This is shown in Figure 5 from 6 hours up to ca. 9 hours of the test and in Figure 6 from 26 hours up to ca. 30 hours of test. For Figure 5, when at the maximum water vapour content of 3 %, the HF content was 1200 ppm, which was achieved when the temperature reached 800 °C. Both the water vapour and HF contents reduced steadily towards respective values of 1.5 % and 600 ppm, before the test was terminated.

For Figure 6, the maximum HF content exceeded 11 000 ppm, which was obtained at a water vapour content of approximately 75 %.

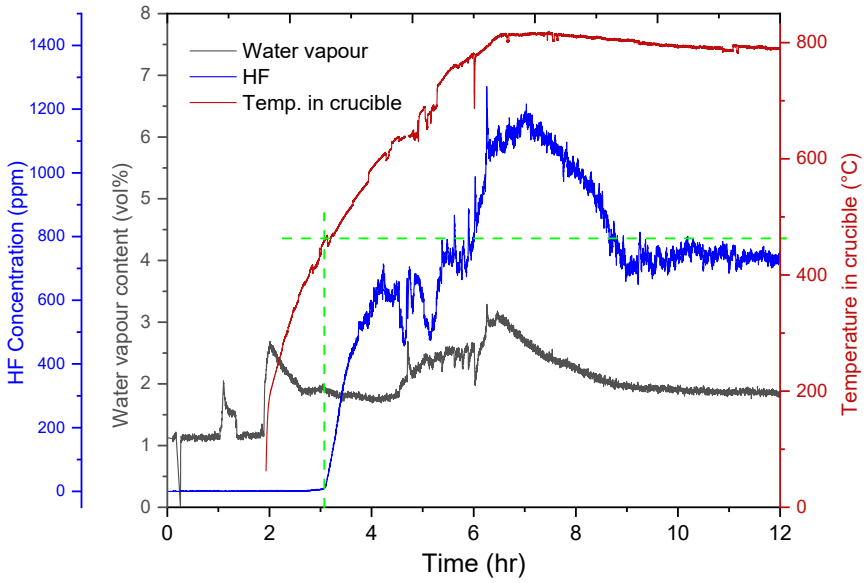

Figure 5. HF, water vapour content and temperature in crucible for the first 12 h of test 1.

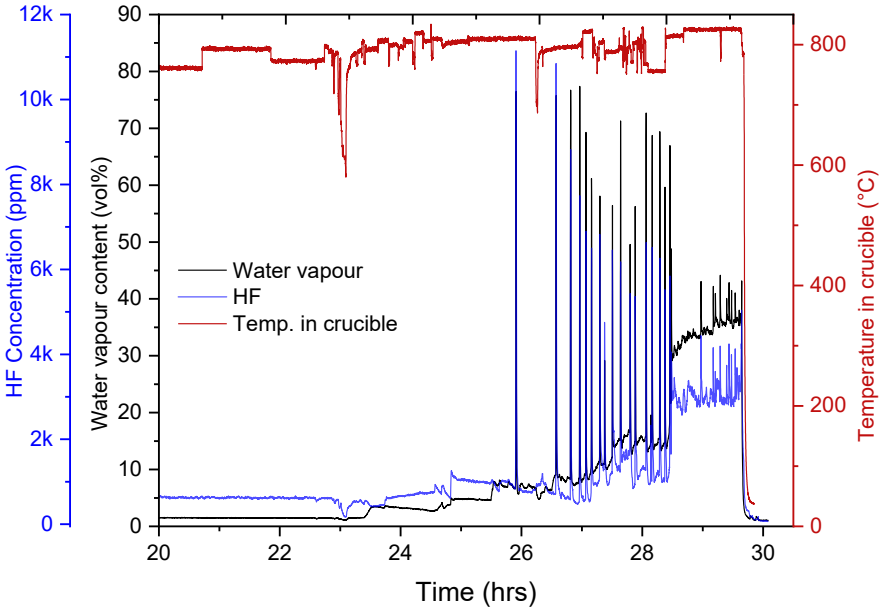

Figure 6. HF, water vapour content, and temperature in crucible data for last 10 hours of test 1, k as in 2k, 4k, etc. on the HF concentration scale stands for 1000.

3.2 Test 2: Melting of Pre-Processed Metal Pad 1

Melting of pre-processed metal pad in an empty pre-heated crucible is shown in Figure 7a. The recovered aluminium and residual bath together with the alumina balls are shown in Figure 7b. The weight of the residual bath and alumina balls were 2.7 kg. The recovered aluminium had a weight of 8.8 kg, which gives an output of 72.5 %.

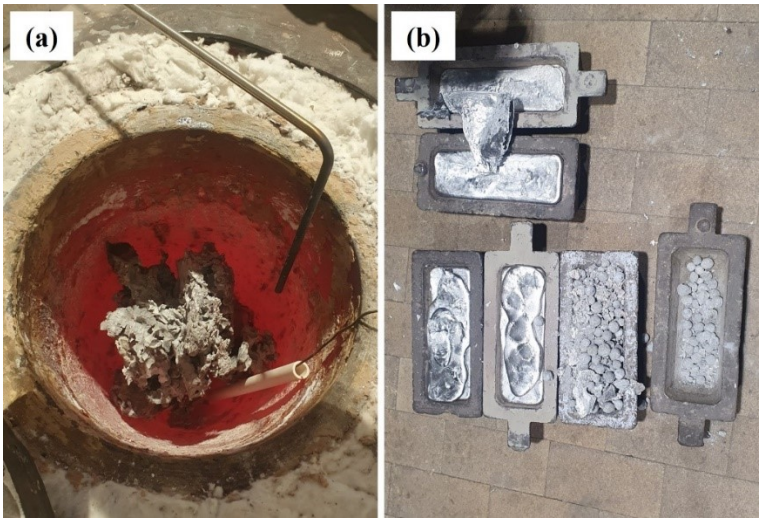

Figure 7. a) Metal pad in crucible just after addition. b) Produced aluminium and residual bath and oxides.

The content of HF and water vapour in the off-gas and the corresponding temperature is shown in Figure 8. It can be observed that the water vapour content increased to approximately 2 % when the metal pad was added, before decreasing and levelling off. The HF content increased as the metal pad was added, reaching a level of about 250 ppm. After the metal pad melted, the HF content was observed to start declining.

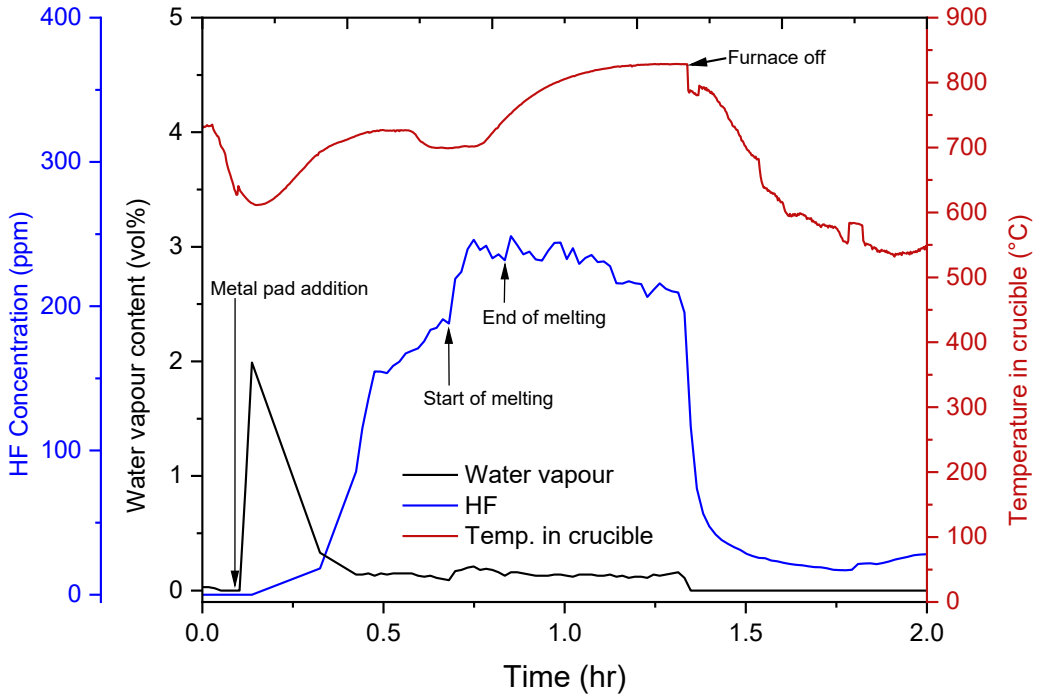

Figure 8. HF, water vapour content and temperature in crucible data for test 2.

3.3 Test 3: Melting of Pre-Processed Metal Pad 2

Results from melting the pre-processed metal pads in pre-melted aluminium are displayed in Figure 9 below. Figures 9c and 9d show dross generated during the melting process. The weight of the dross was 1.2 kg. Figure 9e shows the tapping of the recovered aluminium and pre-melted aluminium from the crucible. The total weight of tapped metal was 74 kg. As the initial molten

aluminium was 60 kg, 14 kg aluminium was recovered from the metal pad, which gave an output of 61.6 %. Figure 9f shows the residue from the melting process which consists of bath components and alumina balls that came with the pre-processed metal pad. Total weight of the residue was 9.7 kg.

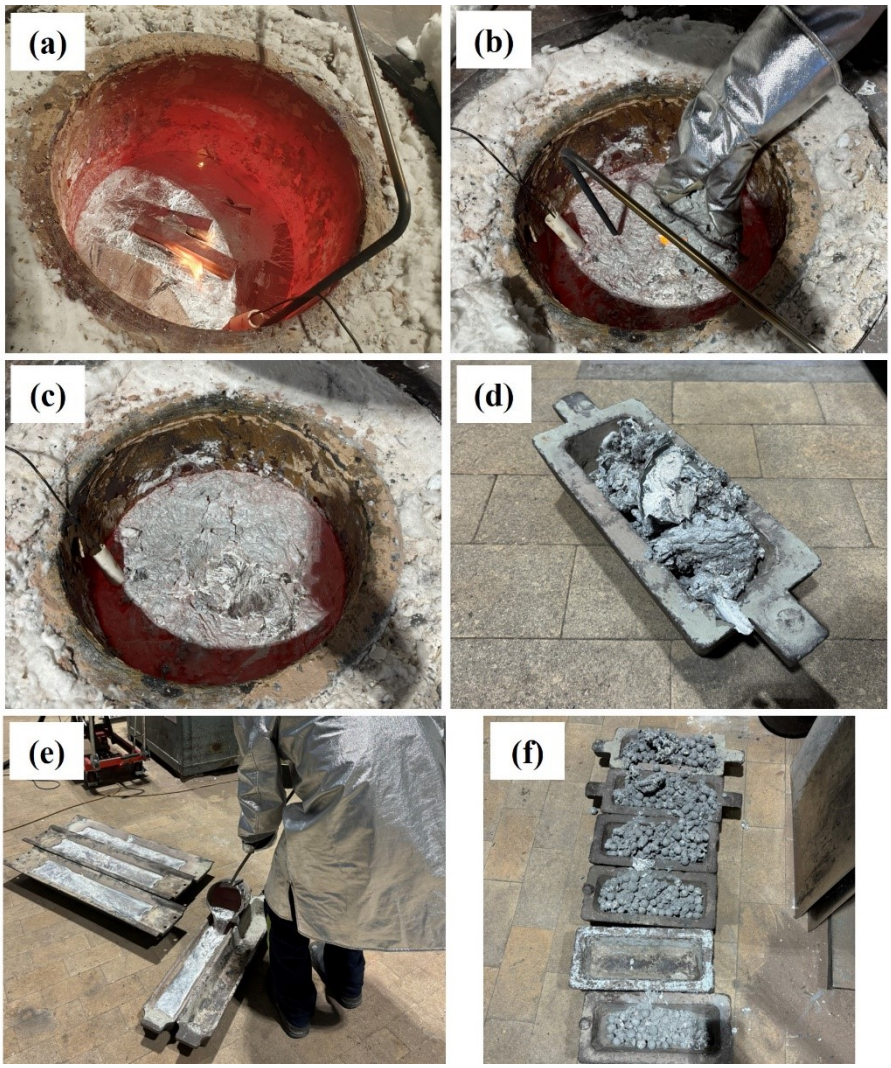

Figure 9. a) Molten aluminium to which the metal pad was added. b) Addition of the metal pad to the molten aluminium. c) Dross formed on the melt. d) Removed dross. e) Tapping aluminium. f) Residual bath and alumina balls.

Figure 10 shows the HF and water vapour content, in addition to the temperature in the crucible, during melting of metal pad in molten aluminium. Initially, the measured HF content was at a baseline of about 10 ppm. When the metal pad was added to the pre-melted aluminium, an increase in both HF and water vapour content was recorded. The highest measured HF content was approximately 170 ppm. Both the HF and water vapour content decreased a few minutes after the metal pad addition.

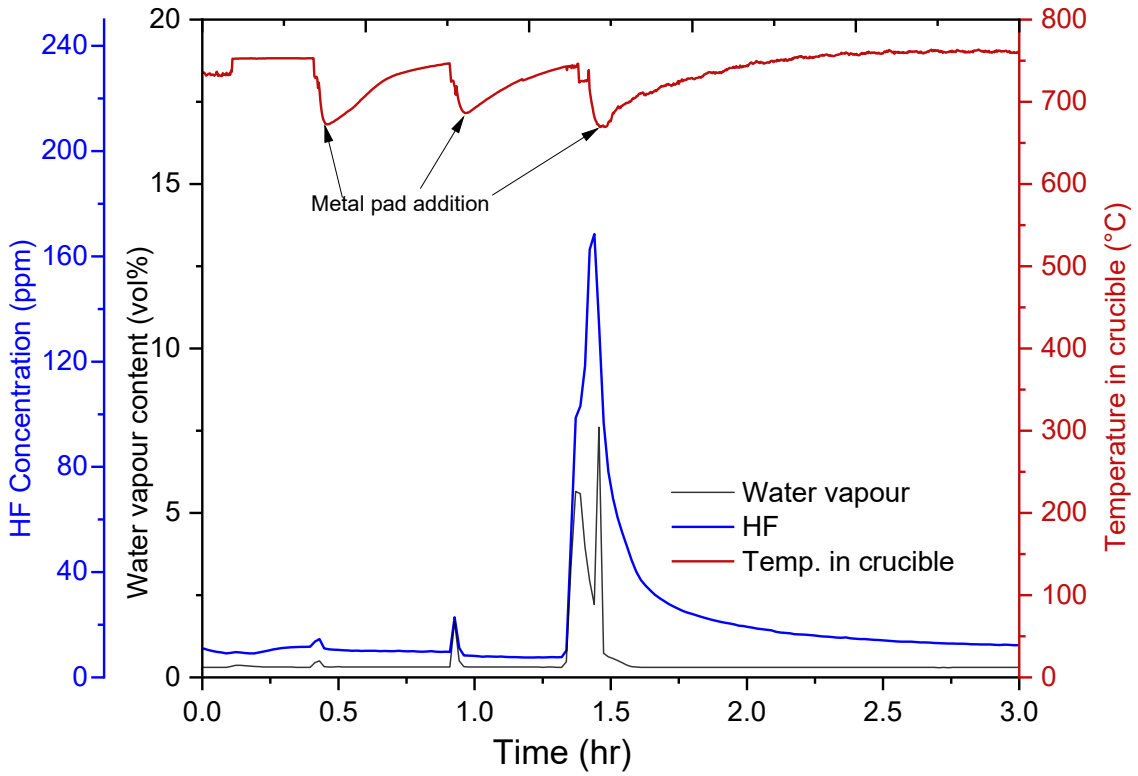

Figure 10. HF, water vapour content and temperature in crucible data for test 3 where the metal pads were immersed in pre-melted aluminium.

3.4 Characterization of Residue from Melting Activities

Results from the powder X-ray diffraction analysis of the bath components collected from the two batches of metal pads from the two smelters showed the same phases. The phases observed are shown by the peaks displayed on the diffractogram referred to as metal pad bath in Figure 11 below. Investigation of the residue collected after the melting process in the different tests also showed the same phases and are indicated by the peaks displayed by the diffractogram labelled residue after melting in Figure 11. The main differences in the phases observed between the metal pad bath and residue after melting are the variations in the cryolite (Na_3AlF_6) and alumina (Al_2O_3) content. The intensity of the peak corresponding to cryolite, which is an indication of the relative content, is observed to decrease in the residue whereas that corresponding to alumina (Al_2O_3) increases. Analysis of the whitish and powdery material seen on the surface of the frozen cryolite showed it was an aluminium oxide containing material with some cryolite. A picture showing the location of the whitish material on the frozen cryolite and its diffractogram is displayed in Figure 12.

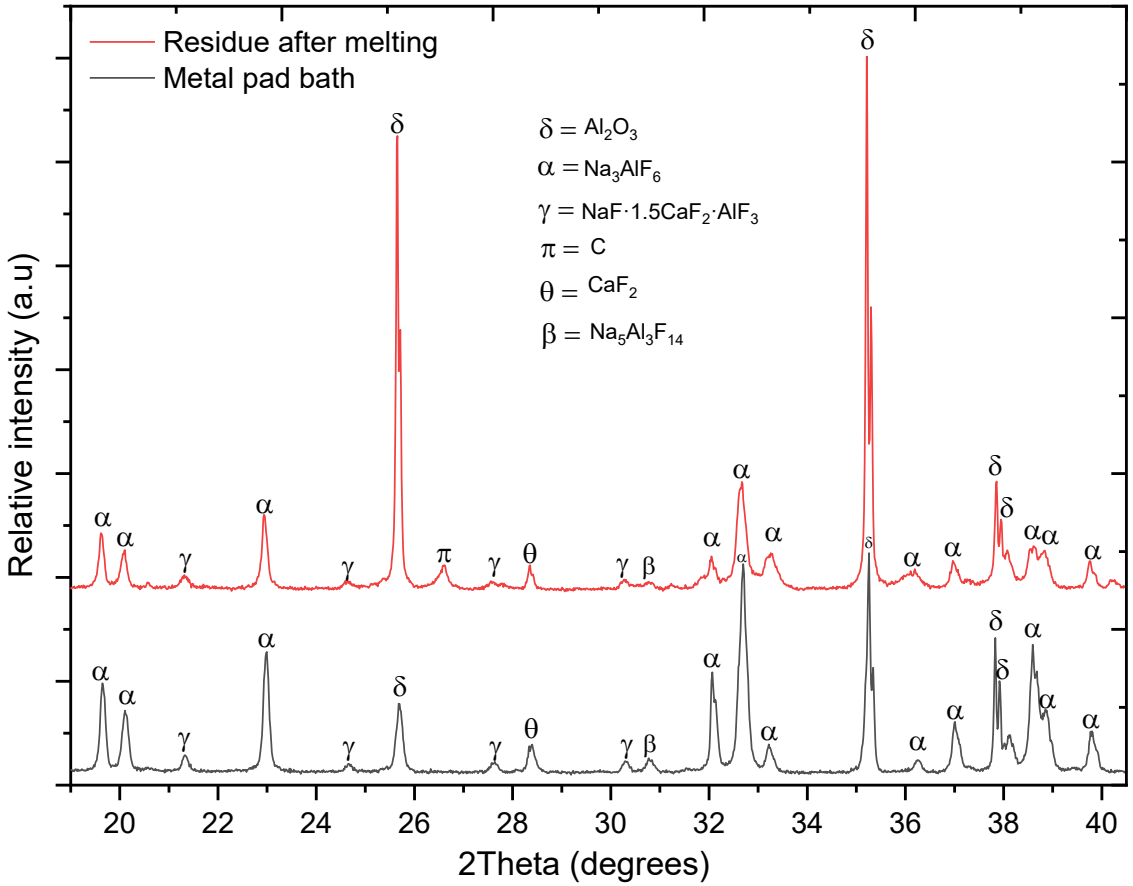

Figure 11. X-ray diffractograms of the metal pad bath and residue after melting.

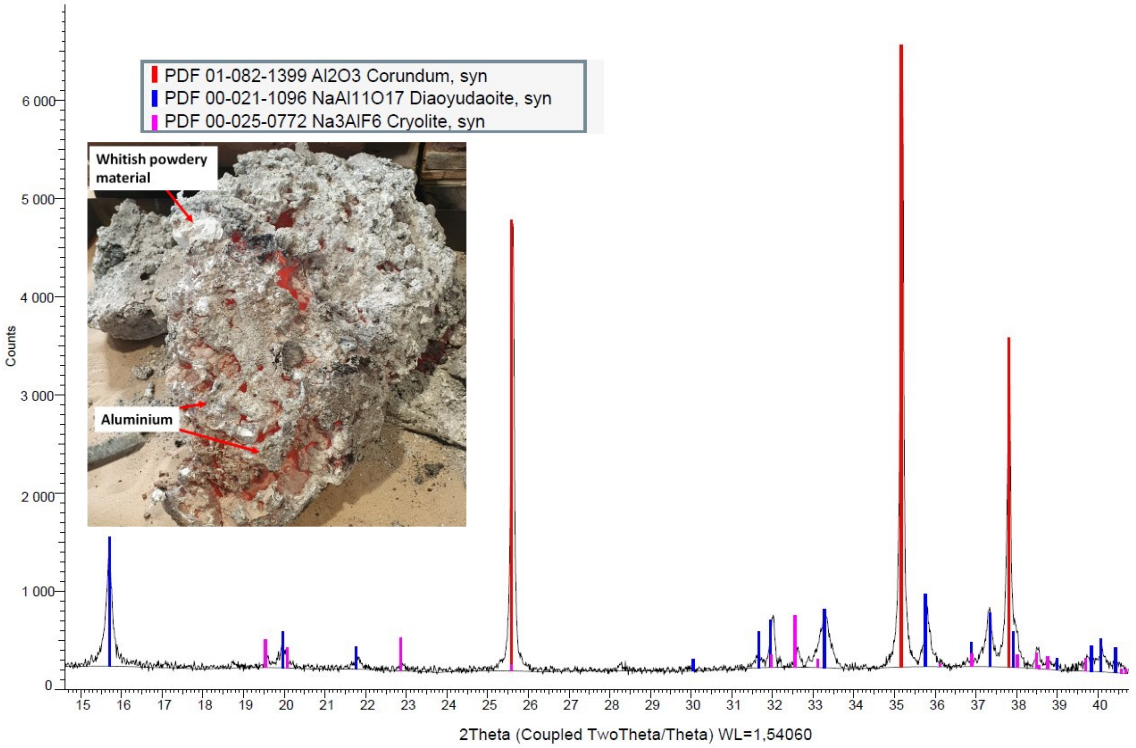

Figure 12. X-ray diffractogram of whitish and powdery material observed during test1. Insert: picture of the frozen cryolite with aluminium and powdery material on the surface.

4. Discussion

4.1 Yield

Results from the melting experiments using the two batches of metal pads where one was pre-processed relative to the other, have shown that pre-processing improves the efficiency of the melting process. Aside the energy wasted in heating the frozen electrolyte that follows the metal pad, the metal melting process takes longer time and may create room for oxidation. The data from experiment 1 which employed the non-pre-processed metal pads showed a very low productivity as only 17.5 kg of aluminium was recovered from a metal pad weighing 74.22 kg, representing ca. 24 % yield. The initial weight of the cryolite part of this metal pad was difficult to determine even though visual observations suggested a higher cryolite content. Also, it can be assumed that there was a relatively high level of oxidation during the melting process. This is because the total weight of the aluminium recovered and residue after melting was higher than the starting metal pad. Furthermore, the XRD diffractogram shown by Figure 12, confirm the formation of an aluminium oxide containing phase that probably resulted from oxidation of the aluminium metal found on the surface of the frozen cryolite. Most likely the extra weight gain is due to the formation of aluminium oxide from the reaction between the molten aluminium and oxygen during the melting process as shown by Equation (1) below.

$$4Al\ (l) + 3O_2 = 2Al_2O_3\ (\text{s}) \quad (1)$$

From Equation 1, it can be assumed that the 2.5 kg weight gained during test 1 was from the oxidation of 2.8 kg of aluminium representing ca. 13.8 % melting loss.

The results from tests 2 and 3, which used pre-processed metal pads, showed relatively higher yields. The two tests gave output yields of 72.5 % and 61.6 %, respectively for test 2 and test 3. Test 3 which involved melting the pre-processed metal pads in pre-melted aluminium had a higher loss due to the formation of dross from the pre-melted aluminium. The output yield was calculated by considering the total amount of metal recovered relative to the total input. Test 3 had the highest input of material due to the contribution from the 60 kg pre-melted aluminium. The decision to melt the metal pads in pre-melted aluminium was taken to reduce oxidation and the formation of HF as was observed during test 1. This is because dipping the metal pads in molten aluminium will reduce access to air and moisture from the environment during the melting process.

4.2 HF Emissions

Formation of HF in the aluminium industry is a well-documented phenomenon due to the fluoride electrolyte employed in the metal production process. The formation of HF is proposed to result from the hydrolysis of the fluoride electrolyte which is mostly cryolite (Na_3AlF_6), by moisture from the atmosphere and within the aluminium oxide feed as given by Equations 2 and 3 [10, 11].

$$H_2O(g) + \frac{2}{3}AlF_3(diss) = \frac{1}{3}Al_2O_3(diss) + 2HF(g) \quad (2)$$

$$H_2O(g) + \frac{2}{3}NaAlF_4(g) = 2HF(g) + \frac{2}{3}NaF(diss) + \frac{1}{3}Al_2O_3(diss) \quad (3)$$

HF emissions were observed for all the three tests. However, it was observed that HF emissions occurred only after the temperature in the crucible had reached a certain level. This is especially true for the first test where the crucible filled with the metal pad was heated from room temperature. During the initial stages of the heating, no HF emissions were recorded even when

moisture was detected. It was after about 3 hours of heating when the temperature reached ca. 450 °C that one could observe HF emission. This is shown in Figure 5. This observation is consistent with the laboratory experiments by Patterson [12] which showed hydrolysis of the fluoride particulates to be only significant at temperatures above 400 °C. Once the right temperature for hydrolysis is reached, HF emission is then dependent on the moisture and fluoride sources. The influence of moisture on HF emission was investigated by using the humidifier to vary the content of moisture and monitoring the corresponding HF emissions during test 1. The results, as can be seen by Figure 6 from ca. 26 hours to 30 hours, confirm the importance of moisture on HF emissions. Also, it was observed that the concentration of HF emitted varied between the non-pre-processed and pre-processed metal pads. The tests using the pre-processed metal pads had the lowest HF emissions relative to the tests with non-pre-processed metal pads which had ca. 5 times higher emissions of HF.

As mentioned above, the HF emissions were higher for the non-pre-processed metal pads probably due to the high frozen cryolite (fluoride) content. However, a difference in HF emission was also observed for the two tests that used the pre-processed metal pads. The HF emission was lowest for the test where the metal pads were immersed in molten aluminium. This is assumed to be due to the reduced exposure to moisture from the environment when the metal pads are immersed.

5. Conclusions

The melting tests have shown that pre-processing of metal pads to reduce the frozen cryolite content has positive effect on both the output and HF emissions. Furthermore, melting the pre-processed metal pads in pre-melted aluminium helps to further reduce the HF emission, however, at the cost of dross formation.

6. Acknowledgement

The present work was financed by the Research Council of Norway (NFR-nr 327564) and done in cooperation with Alcoa Norway, Hydro Aluminium, and Speira. The industry partners also provided materials for the tests. Permission to publish the results is gratefully acknowledged.

7. References

1. International Aluminium Institute, Primary Aluminium Production, https://international-aluminium.org/. (Accessed on 20th May 2024).
2. Jomar Thonstad et al., *Aluminium Electrolysis: Fundamentals of the Hall-Héroult Process*, 3rd Edition, Dusseldorf, Aluminium-Verlag, 2001.
3. Halvor Kvande, Per Arne Drabløs, The Aluminum Smelting Process and Innovative Alternative Technologies, *JOEM* 56, 2014, S23–S32.
4. Kai Grjotheim and Halvor Kvande, *Introduction to Aluminium Electrolysis: Understanding the Hall-Héroult Process,* 2nd Edition, Dusseldorf, Aluminium-Verlag, 1993.
5. Samuel Senanu, *Cathode Wear in Aluminium Electrolysis Cells*, PhD Thesis, Norwegian University of Science and Technology, Trondheim, Norway, 2019.
6. Morten Sørlie and Harald A. Øye, *Cathodes in aluminium electrolysis*, 3rd Edition, Düsseldorf Aluminium-Verlag, 2010, 662 pages.
7. M. Sørlie, J. Hvistendahl and H.A. Øye, Early Failure Mechanisms in Aluminum Cell Cathodes, *Light Metals* 1993, 299–308.
8. Samuel Senanu et al., Cathode Wear Based on Autopsy of a Shutdown Aluminium Electrolysis Cell, *Light Metals* 2017, 561–570.
9. Alton T. Tabereaux, The Survivability of Aluminum Potlines After Lengthy Electrical Power Outages, *Light Metals* 2022, 448-457.

10. Thor Anders Aarhaug and Arne Petter Ratvik, Aluminium Primary Production Off-Gas Composition and Emissions: An Overview, *JOM* 71(9), 2019, 2966–2977.
11. Camilla Sommerseth et al., Correlation between Moisture and HF Formation in the Aluminium Process, *Light Metals* 2011, 339–344.
12. Edwin Campbell Patterson, *Hydrogen Fluoride Emissions from Aluminium Electrolysis Cells,* PhD Thesis, University of Auckland, Auckland, New Zealand, 2002.